



OPEN

SUBJECT AREAS:
METALS AND ALLOYS
STRUCTURAL PROPERTIES

A Promising New Class of High-Temperature Alloys: Eutectic High-Entropy Alloys

Yiping Lu^{1,2}, Yong Dong¹, Sheng Guo³, Li Jiang¹, Huijun Kang¹, Tongmin Wang⁴, Bin Wen², Zhijun Wang^{5,6}, Jinchuan Jie¹, Zhiqiang Cao¹, Haihui Ruan⁷ & Tingju Li^{1,8}Received
29 April 2014Accepted
5 August 2014Published
27 August 2014

Correspondence and requests for materials should be addressed to Y.L. (luyiping@dlut.edu.cn); S.G. (sheng.guo@chalmers.se) or T.W. (tmwang@dlut.edu.cn)

¹School of Materials Science and Engineering, Dalian University of Technology, Dalian 116024, China, ²State Key Laboratory of Metastable Materials Science and Technology, Yanshan University, Qinhuangdao, 066004, China, ³Surface and Microstructure Engineering Group, Materials and Manufacturing Technology, Chalmers University of Technology, SE-41296, Gothenburg, Sweden, ⁴Key Laboratory of Materials Modification by Laser, Ion, and Electron Beams, Ministry of Education, Dalian University of Technology, Dalian 116024, China, ⁵Department of Mechanical and Biomedical Engineering, City University of Hong Kong, Kowloon, Hong Kong, China, ⁶State Key Laboratory of Solidification Processing, Northwestern Polytechnical University, Xi'an 710072, China, ⁷Department of Mechanical Engineering, The Hong Kong Polytechnic University, Hung Hom, Hong Kong, China, ⁸State Key Laboratory of Structural Analysis for Industrial Equipment, Dalian University of Technology, Dalian 116024, China.

High-entropy alloys (HEAs) can have either high strength or high ductility, and a simultaneous achievement of both still constitutes a tough challenge. The inferior castability and compositional segregation of HEAs are also obstacles for their technological applications. To tackle these problems, here we proposed a novel strategy to design HEAs using the eutectic alloy concept, i.e. to achieve a microstructure composed of alternating soft fcc and hard bcc phases. As a manifestation of this concept, an AlCoCrFeNi_{2.1} (atomic portion) eutectic high-entropy alloy (EHEA) was designed. The as-cast EHEA possessed a fine lamellar fcc/B2 microstructure, and showed an unprecedented combination of high tensile ductility and high fracture strength at room temperature. The excellent mechanical properties could be kept up to 700 °C. This new alloy design strategy can be readily adapted to large-scale industrial production of HEAs with simultaneous high fracture strength and high ductility.

High-entropy alloys (HEAs), or multi-principal-element alloys, emerge as a new research frontier in the metallic materials community^{1–6}. HEAs differentiate with conventional alloys in that they have at least four principal elements, instead of one or two in the latter. It is a breakthrough to the alloy design in the traditional physical metallurgy, and it opens a new arena for explorations of new materials and new properties. Previous studies have indicated that HEAs have a high softening resistance at elevated temperatures^{5,7}, and sluggish diffusion kinetics⁸. Therefore, HEAs are widely regarded as highly promising high-temperature materials. Before the high-temperature application of HEAs can be seriously pursued, a technical challenge in terms of the mechanical property needs to be tackled. Basically, single-phased HEAs have been found difficult to reach a reasonable balance between strength and (tensile) ductility^{1,2}. Single-phased fcc structured HEAs are ductile but not strong enough^{9,10}. Single-phased bcc structured HEAs, on the other hand, can be very strong but at the price of brittleness¹¹. To the best of our knowledge, there is no report of HEAs possessing an excellent balanced strength and tensile ductility. Naturally, a composite way can be expected to achieve this balance. However, simply introducing a combination of fcc and bcc phases, without a proper structural design, could not solve the problem¹². Moreover, the inferior castability and compositional segregation, which are common for HEAs, further downgrade their mechanical properties and cast shadow on their engineering applications^{3,4}.

In order to address to these important technical issues that HEAs are currently facing, we proposed here to use the eutectic alloy idea to design HEAs with the composite structure, or it can be said to use the high-entropy alloy concept to design eutectic alloys. Furthermore, we proposed to design the eutectic alloys with a mixture of soft fcc and hard bcc phases, to achieve the balance of high fracture strength and high ductility. Apart from being a new way to obtain the composite structure in HEAs, eutectic alloys are also known to be good candidate high-temperature alloys, because the eutectic solidification structure has the following features: 1) near-equilibrium microstructures that resist change at temperatures as high as their reaction temperature; 2) low-energy phase boundaries; 3) controllable microstructures; 4) high rupture strength; 5) stable defect structures; 6) good high-

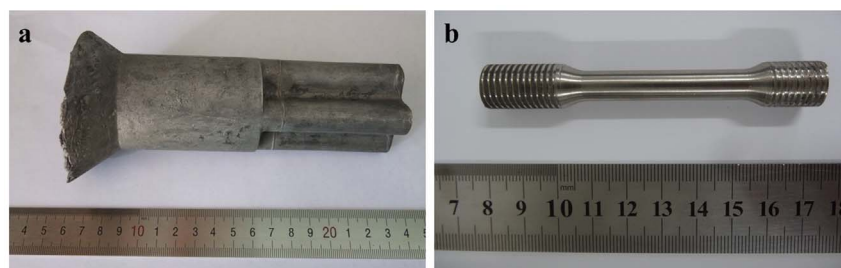


Figure 1 | Macrograph. (a), The bulk AlCoCrFeNi_{2.1} EHEA ingot. (b), The tensile test specimen cut from the ingot.

temperature creep resistance; 7) regular lamellar or rod-like eutectic organization, forming an in-situ composite¹³. In addition, eutectic alloys are known to have better castability. Also importantly, since the eutectic reaction is an isothermal transformation and hence there exists no a solidification temperature range, both the segregation and shrinkage cavity can be alleviated. Accordingly, if eutectic HEAs with the composite fcc/bcc structure can be prepared, they are expected to possess the advantageous mechanical properties and castability of eutectic alloys, clearing obstacles for their technological application.

Results

Microstructure and phase constitution. To verify this novel alloy design strategy, an industrial scale AlCoCrFeNi_{2.1} ingot of ~2.5 kg in weight was prepared, as shown in Fig. 1a. The bulk AlCoCrFeNi_{2.1}

alloy exhibited an excellent castability with few casting defects, significantly differentiating with other bulk HEAs. The tensile test specimen was machined from the bulk alloy ingot and is shown in Fig. 1b. The cast microstructure of AlCoCrFeNi_{2.1} is shown in Fig. 2a. Even in such a bulk cast ingot, a uniform and fine lamellar microstructure characteristic of eutectic alloys was achieved. The interlamellar spacing was about 2 μm. The coupled grown two phases showed a clear compositional contrast, with the regions marked by *A* in Fig. 2b were rich in Co, Cr and Fe, while the regions marked by *B* were rich in Al and Ni (detailed compositional information given in Table 1). An enlarged microstructure given in Fig. 2c shows that dense nanoscale NiAl-rich precipitates (marked as B_{II}) occurred in the CoCrFe-rich region. The X-ray diffraction (XRD) pattern of the alloy is given in Fig. 3a, showing an fcc/B2 dual-phase constitution. The differential scanning calorimetric (DSC) curve given in Fig. 3b shows only one melting event, further evidencing the eutectic composition in this alloy. Correlating the compositional information and the XRD result, the *A* regions shall correspond to the fcc phase while the *B* regions (including B_{II}) to the B2 phase.

Tensile properties. The eutectic AlCoCrFeNi_{2.1} alloy, with an fcc/B2 dual-phase constitution and a uniform and fine lamellar microstructure, exhibited the combination of both high fracture strength and high ductility, which has never been achieved in previously reported HEAs¹. The room temperature tensile test showed a fracture stress of 944 MPa and an elongation of 25.6%, from the engineering stress-strain curve given in Fig. 4a. These values converted to 1186 MPa and 22.8% in the true stress/strain condition. Noteworthy, this alloy exhibited an ultra-high strain hardening behavior, having the proof stress (the proof stress is determined by shifting the linear elastic curve to 0.2% strain. We choose to not to call it the yield stress, as the mechanism for such a low elastic limit is still unclear at this stage.) of 75 MPa but reaching the fracture stress close to 1.2 GPa. At elevated temperatures of 600 and 700 °C (Fig. 4b), the proof stress, fracture stress and elongation were 95 MPa, 806 MPa, 33.7%, and 108 MPa, 538 MPa, 22.9%, respectively, both in the true stress/strain condition. The combination of high strength and high ductility for this EHEA could be maintained at least up to 700 °C. The mechanical properties of the as-cast EHEA can be further tuned by thermo-mechanical treatments. Figure 5 shows that a simple cold rolling with a thick reduction of 8% can increase the engineering/true proof stress and fracture stress to 275 MPa and 1145 MPa/

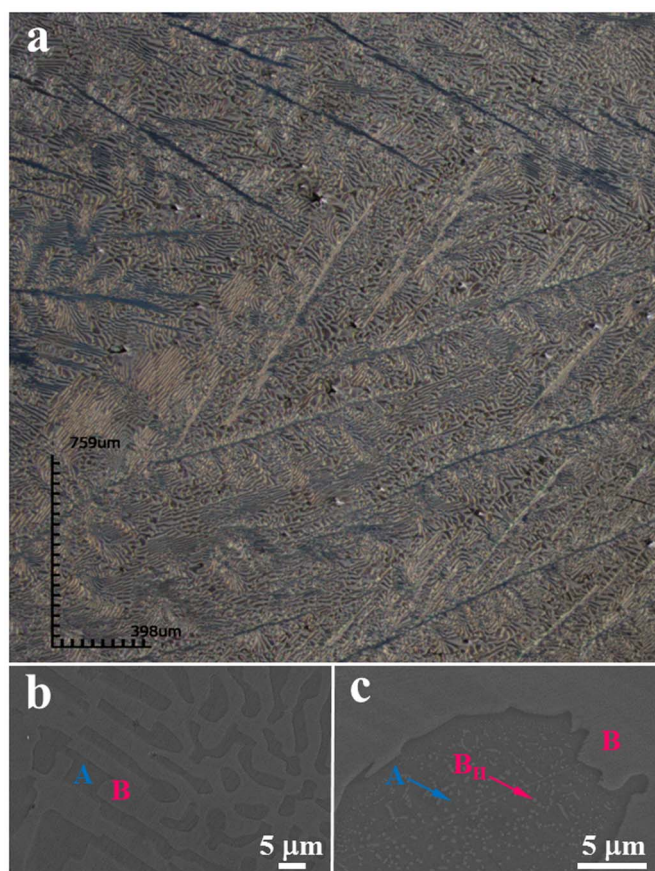


Figure 2 | Micrograph. (a), An LSCM image showing the eutectic microstructure of the AlCoCrFeNi_{2.1} alloy. (b), The lamellar dual-phase structure seen under SEM. (c), the enlarged view showing the precipitates in one phase. Symbols *A* and *B* in (b) and (c) represent two compositionally different phases. B_{II} phase in (c) has the same composition of *B* phase, but is marked so to differentiate with the eutectic *B* phase.

Table 1 | EDS analyses of the constituent phases in the eutectic structure

	Elements (at. %)				
	Al	Co	Cr	Fe	Ni
Nominal	16.39	16.39	16.39	16.39	34.43
Region A	11.06	18.01	21.23	19.44	30.26
Region B	29.73	12.38	10.25	10.84	36.80

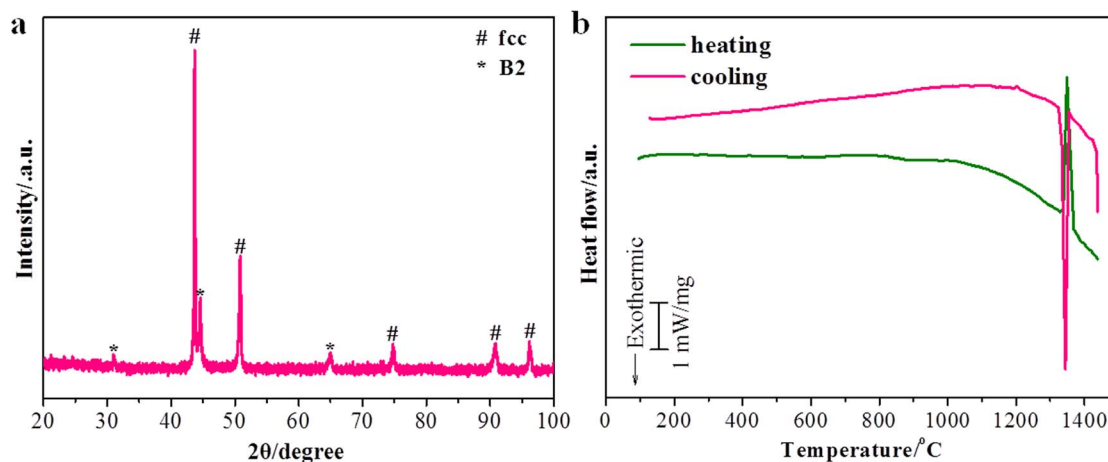


Figure 3 | Phase constitution and thermal behavior for the AlCoCrFeNi_{2.1} alloy. (a), the XRD pattern. (b), The DSC curve.

1265 MPa, respectively, while remaining a decent ductility of 10.4%/9.9% in elongation.

Technical advantages over conventional high-temperature alloys.

To further showcase the excellent balanced mechanical properties of this newly developed EHEA as candidate high-temperature alloys, a comparison between it and NiAl and NiAl/Cr(Mo) eutectic alloys^{14–26} is given in Fig. 6. The reference alloys were chosen because the current EHEA can be regarded as a highly concentrated pseudo-binary NiAl/(Co, Cr, Fe) eutectic alloy, and they are also known to be promising high-temperature alloys, due to the lower density and melting point, much higher thermal conductivity, and excellent oxidation resistance at high temperatures²⁶. The major disadvantages for NiAl are the low ductility at room temperature and the low strength at high-temperatures²⁶, which also constitute the motivation to develop NiAl/Cr(Mo) eutectic alloys, where the in-situ formed composite structure is expected to improve the mechanical properties of NiAl. As seen in Fig. 6a, compared to NiAl or NiAl/Cr(Mo) eutectic alloys, the EHEA exhibited a much higher fracture strength, and more importantly, a simultaneously much higher ductility at room temperature. Considering the preparation of NiAl and NiAl/Cr(Mo) eutectic alloys often require the expensive processing routes like single crystal growth, directional solidification, and various thermomechanical treatments, that the EHEA prepared using conventional casting and without subsequent processing can have such excellent mechanical

properties is indeed groundbreaking. As shown in Fig. 6b, the higher strength of the EHEA over non-EHEAs can be kept at least to 700°C. It is stressed here that the density of this EHEA was measured to be 7.38 g/cm³, much lower than those of Ni-based superalloys typically with a density of above 8.0 g/cm³. Further optimization of the room-temperature and elevated temperature properties while maintaining this relatively lower density, will certainly enable EHEAs to become competitive high-temperature alloys to Ni-based superalloys. The extraordinary work hardening behavior of the EHEA is reflected when comparing with NiAl-based alloys (Fig. 6c), where the ratios of fracture strength to yield strength ($\sigma_{UTS}/\sigma_{0.2}$) are normally in the range of 1 ~ 2^{14–26}, while the EHEA has a $\sigma_{UTS}/\sigma_{0.2}$ (note it is the proof stress here) close to 16. Such a high $\sigma_{UTS}/\sigma_{0.2}$ is also far beyond those of conventional alloys, which are in the range of 1 ~ 3^{27–29}. The unprecedentedly large strain hardening and low yield stress (proof stress) give rise to the unique opportunity of this EHEA in producing ultrahigh strength components after large plastic deformation, which was exemplified by the results given in Fig. 5 and still awaits further investigations. The very large strain hardening for the as-cast EHEA could originate from the fine regular lamellar structure that easily stores dislocations³⁰ and the alternating soft fcc phases and hard B2-structured NiAl-rich phases. When dislocations pass through soft fcc phases, these hard B2 phases, including the nanoscale B2-structured precipitates within the fcc phases, could pin the movement of dislocations and result in the significant work hardening phenomenon.

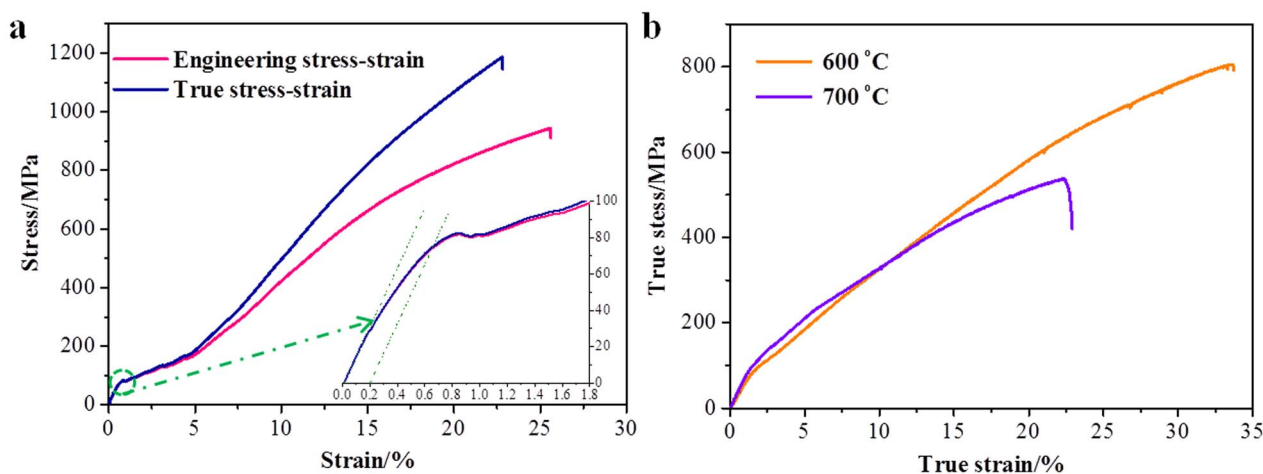


Figure 4 | Tensile stress-strain curves for the AlCoCrFeNi_{2.1} alloy. (a), Room-temperature curves. (b), True tensile stress-strain curves tested at 600 and 700°C, respectively.

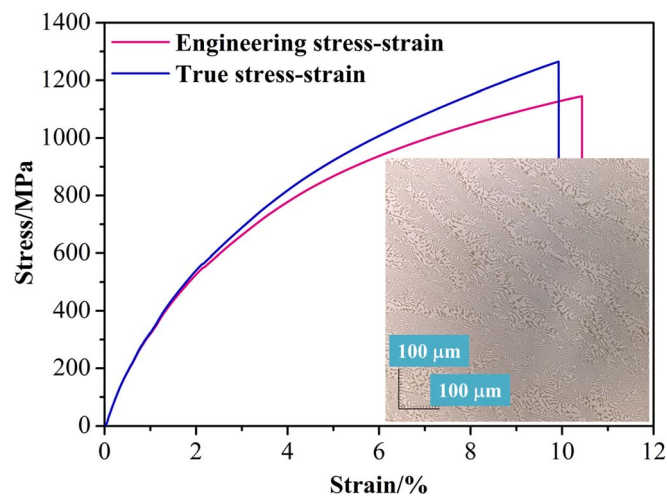


Figure 5 | Tensile stress-strain curves for the 8% cold rolled AlCoCrFeNi_{2.1} alloy. The inset shows the microstructure of the cold rolled material.

Discussion

As such, our alloy design strategy resulted in the discovery of an EHEA with a fine lamellar fcc/B2 structure and balanced high fracture strength and high ductility. This novel strategy is promising to solve the problems inhibiting the engineering application of HEAs as high-temperature materials, including the inferior castability and compositional segregation, and the conflict between high fracture strength and high ductility. In addition, this novel strategy also brought breakthrough to NiAl-based alloys in significantly enhancing the ductility at room temperature while simultaneously achieving the high strength. The EHEA concept, combining the advantages of both HEAs and eutectic alloys, and at the same time eliminating the disadvantages of these two types of alloys, leads to a promising new class of high-temperature alloys. Using this new alloy design strategy, an industrial scale HEA with uniform organizations and compositions can be prepared by the conventional casting method in a low cost way, allowing for large-scale industrial applications. Further exploration of new EHEAs will be based on previous established physical metallurgy principles to design HEAs, utilizing physiochemical material properties including atomic radius, mixing enthalpy and valence electron concentration^{2,31–33}. Eutectic alloys compositions can be pinpointed assuming a pseudo-binary multi-component alloy system, and then varying the concentration of one element systematically³³. Thermodynamics calculations based on the CALPHAD (calculation of phase diagrams) method can also provide an insightful guidance to design EHEAs^{34–35}, on the premise that reliable thermodynamics database for HEAs are to be established and completed.

In summary, here we proposed a novel strategy to design high-entropy alloys (HEAs), i.e., the concept of eutectic high-entropy alloys (EHEAs), to solve the challenging issues for this new type of advanced metallic materials, including the conflict between high fracture strength and high ductility, and the inferior castability and compositional segregation. Based on the new strategy, we successfully designed a highly uniform AlCoCrFeNi_{2.1} EHEA, with an unprecedented combination of castability, high fracture strength and high ductility. The bulk EHEA ingot of ~2.5 kg in weight was prepared by the conventional casting method using the commercially pure raw materials. The EHEA exhibited a fine lamellar microstructure consisting of coupled grown fcc/B2 phases. Our design strategy is of great significance in both scientific and technical aspects, and can be readily adapted to large-scale industrial production of HEAs.

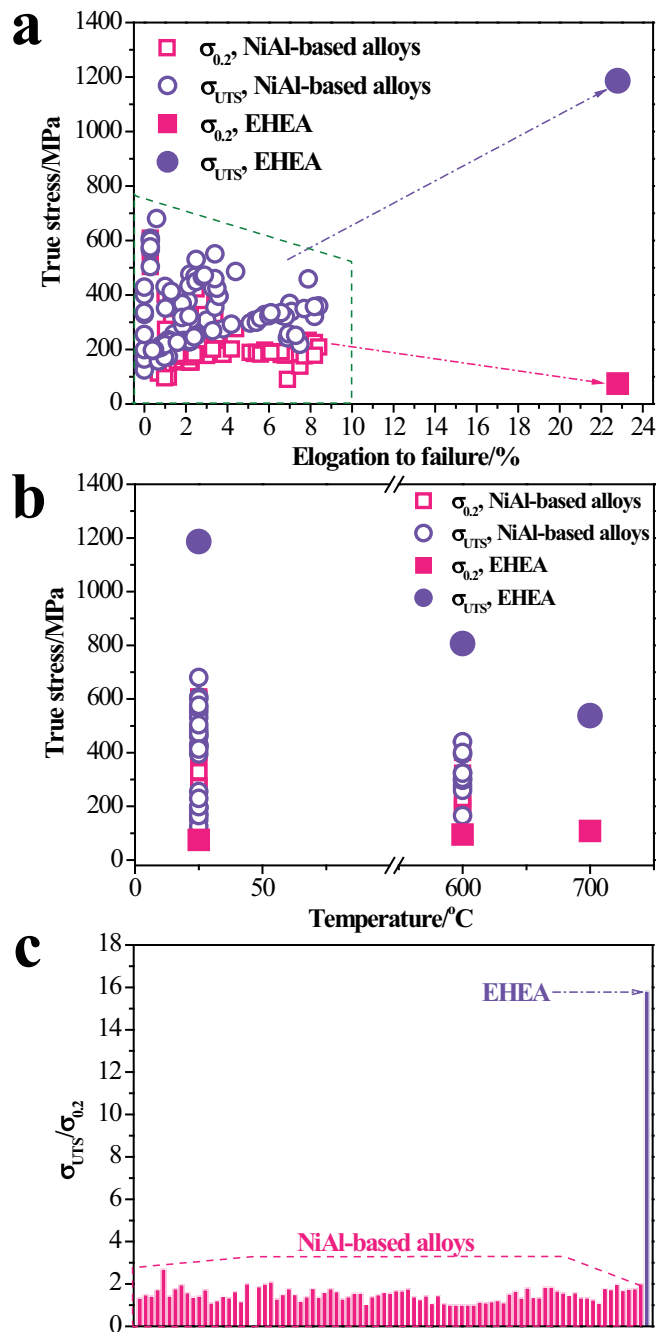


Figure 6 | Comparison of mechanical properties. (a), The comparison of room-temperature tensile mechanical properties. (b), The comparison of high-temperature strength. (c), The comparison of the ratio of fracture stress to yield stress (proof stress), between the AlCoCrFeNi_{2.1} EHEA and non-EHEAs, comprising NiAl-base alloys.

Methods

The master alloy of AlCoCrFeNi_{2.1} was prepared from commercially pure elements (Al, Co, Ni: 99.9 wt.%; Cr, Fe: 99.5 ~ 99.6 wt.%). The raw elements were alloyed in a BN crucible in the vacuum induction melting furnace. The BN crucible was heated to 600°C and held for 1 hour to remove the water vapor, before putting into the furnace. The pouring temperature was set to be 1500°C. Approximately 2.5 kg of master alloys were melted, superheated and poured into a MgO crucible with the length of 220 mm, upper inner diameter of 62 mm and bottom inner diameter of 50 mm. In all cases, the furnace chamber was first evacuated to 6×10^{-2} Pa and then backfilled with high-purity argon gas to reach 0.06 MPa. An IRTM-2CK infrared pyrometer was employed to monitor the temperature with an absolute accuracy of $\pm 2^\circ\text{C}$. The microstructure and composition of the alloy were investigated by laser scanning confocal microscope (LSCM), and scanning electron microscope (SEM, Zeiss Supra 55) equipped with an attached X-ray energy dispersive spectrometer (EDS). The



phase constitution of the alloy was characterized by the X-ray diffractometer (XRD, Shimadzu XRD-6000) using a Cu target, with the scanning rate of $4^\circ/\text{min}$ and the 2θ scanning range of $20^\circ\text{--}100^\circ$. The differential scanning calorimetry (DSC, Netzsch STA 449 F3) curve of the alloy was measured from ambient temperature to 1450°C , during both the heating and cooling process, under the protection of a flow argon gas and the heating/cooling rate used was 10 K/min . Room-temperature tensile tests were performed using the Instron 5569 testing machine at a constant strain rate of $1 \times 10^{-3}\text{ s}^{-1}$. The tensile test specimens cut from as-cast alloys had a diameter of 8 mm and gauge length of 40 mm. High-temperature tensile tests were conducted on a Gleeble 3500 system at a strain rate of $1 \times 10^{-3}\text{ s}^{-1}$. In all high-temperature tensile tests, the chamber was first evacuated to 30 Pa and backfilled with high-purity argon gas to reach 0.05 MPa. Tensile tests were also carried out for cold rolled specimens. Plates of the dimension of 100 mm (length) \times 16 mm (width) \times 10 mm (thickness) were machined from the as-cast alloys, and they were sequentially cold rolled with ultimately a thick reduction of 8%. Specimens with a gauge length of 40 mm and a thickness of 3 mm were subject to the room temperature tensile tests, at a strain rate of $2 \times 10^{-3}\text{ s}^{-1}$. For the microstructural observations, the alloy was sequentially polished and etched with the 10 vol. % aqua regia - 90 vol. % ethanol solution at room temperature. The density of the cast alloy was measured following the Archimedes' principle, using the Metter Toledo XS64 density measurement unit.

- Zhang, Y. *et al.* Microstructures and properties of high-entropy alloys. *Prog. Mater. Sci.* **61**, 1–93 (2014).
- Guo, S., Ng, C., Lu, J. & Liu, C. T. Effect of valence electron concentration on stability of fcc or bcc phase in high entropy alloys. *J. Appl. Phys.* **109**, 103505 (2011).
- Hemphill, M. A. *et al.* Fatigue behavior of $\text{Al}_{0.5}\text{CoCrCuFeNi}$ high entropy alloys. *Acta Mater.* **60**, 5723–5734 (2012).
- Tong, C. J. *et al.* Microstructure characterization of $\text{Al}_x\text{CoCrCuFeNi}$ high-entropy alloy system with multiprincipal elements. *Metall. Mater. Trans. A* **36**, 881–893 (2005).
- Yeh, J. W. *et al.* Nanostructured high-entropy alloys with multiple principal elements: Novel alloy design concepts and outcomes. *Adv. Eng. Mater.* **6**, 299–303 (2004).
- Cantor, B., Chang, I. T. H., Knight, P. & Vincent, A. J. B. Microstructural development in equiatomic multicomponent alloys. *Mater. Sci. Eng. A* **375–377**, 213–218 (2004).
- Hsu, C. Y. *et al.* On the superior hot hardness and softening resistance of $\text{AlCoCr}_x\text{FeMo}_{0.5}\text{Ni}$ high-entropy alloys. *Mater. Sci. Eng. A* **528**, 3581–3588 (2011).
- Tsai, K. Y., Tsai, M. H. & Yeh, J. W. Sluggish diffusion in Co–Cr–Fe–Mn–Ni high-entropy alloys. *Acta Mater.* **61**, 4887–4897 (2013).
- Wang, F. J., Zhang, Y., Chen, G. L. & Davies, H. A. Tensile and compressive mechanical behavior of a $\text{CoCrCuFeNiAl}_{0.5}$ high entropy alloy. *Int. J. Mod. Phys. B* **23**, 1254–1259 (2009).
- Otto, F. *et al.* The influences of temperature and microstructure on the tensile properties of a CoCrFeMnNi high-entropy alloy. *Acta Mater.* **61**, 5743–5755 (2013).
- Senkov, O. N., Wilks, G. B., Miracle, D. B., Chuang, C. P. & Liaw, P. K. Refractory high-entropy alloys. *Intermetallics* **18**, 1758–1765 (2010).
- Kuznetsov, A. V., Shaysultanov, D. G., Stepanov, N. D., Salishchev, G. A. & Senkov, O. N. Tensile properties of an AlCrCuNiFeCo high-entropy alloy in as-cast and wrought conditions. *Mater. Sci. Eng. A* **533**, 107–118 (2012).
- Glicksman, M. E. *Principles of Solidification: An Introduction to Modern Casting and Crystal Growth Concepts* (Springer Verlag, New York, 2010).
- Liang, Y. C. *et al.* Effect of growth rate on the tensile properties of DS NiAl/Cr(Mo) eutectic alloy produced by liquid metal cooling technique. *Intermetallics* **18**, 319–323 (2010).
- George, E. P. & Liu, C. T. Brittle fracture and grain boundary chemistry of microalloyed NiAl. *J. Mater. Res.* **5**, 754–762 (1990).
- Ishida, K., Kainuma, R., Ueno, N. & Nishizawa, T. Ductility enhancement in NiAl (B2)-base alloys by microstructural control. *Metall. Trans. A* **22**, 441–446 (1991).
- Schneibel, J. H., Darolia, R., Lahrman, D. F. & Schmauder, S. Fracture morphology of NiAl single-crystals tested in tension. *Metall. Trans. A* **24**, 1363–1371 (1993).
- Yang, Y. M., Jeng, S. M., Bain, K. & Amato, R. A. Microstructure and mechanical behavior of in-situ directional solidified NiAl/Cr(Mo) eutectic composite. *Acta Mater.* **45**, 295–308 (1997).
- Guo, J. T., Xie, Y., Sheng, L. Y., Zhou, L. Z. & Liang, Y. C. Effect of withdrawal rate on microstructure and mechanical properties of a directionally solidified NiAl-based hypoeutectic alloy doped with trace Hf and Ho. *Intermetallics* **19**, 206–211 (2011).
- Rosas, G., Esparza, R., Bedolla, A. & Perez, R. Tensile strength and ductility of Al–MT (MT = Fe, Ni) intermetallic alloys. *Mater. Manuf. Process.* **22**, 305–309 (2007).
- Cui, C. Y., Guo, J. T., Qi, Y. H. & Ye, H. Q. Deformation behavior and microstructure of DS NiAl/Cr(Mo) alloy containing Hf. *Intermetallics* **10**, 1001–1009 (2002).
- Guo, J. T., Cui, C. Y., Chen, Y. X., Li, D. X. & Ye, H. Q. Microstructure, interface and mechanical property of the DS NiAl/Cr(Mo,Hf) composite. *Intermetallics* **9**, 287–297 (2001).
- Cui, C. Y., Chen, Y. X., Guo, J. T., Li, D. X. & Ye, H. Q. Preliminary investigation of directionally solidified NiAl-28Cr-5.5Mo-0.5Hf composite. *Mater. Lett.* **43**, 303–308 (2000).
- Weaver, M. L., Noebe, R. D., Lewandowski, J. J., Oliver, B. F. & Kaufman, M. J. The effects of interstitial content, heat-treatment, and prestrain on the tensile properties of NiAl. *Mater. Sci. Eng. A* **192**, 179–185 (1995).
- Darolia, R. & Walston, W. S. Effect of specimen surface preparation on room temperature tensile ductility of an Fe-containing NiAl single crystal alloy. *Intermetallics* **4**, 505–516 (1996).
- Bogner, S. *et al.* Microstructure of a eutectic NiAl–Mo alloy directionally solidified using an industrial scale and a laboratory scale Bridgman furnace. *Int. J. Mater. Res.* **103**, 17–23 (2012).
- Bannister, A. C., Ochoa, J. R. & Gutierrez-Solana, F. Implications of the yield stress/tensile stress ratio to the SINTAP failure assessment diagrams for homogeneous materials. *Eng. Fract. Mech.* **67**, 547–562 (2000).
- Yamanaka, K., Mori, M., Kuramoto, K. & Chiba, A. Development of new Co–Cr–W-based biomedical alloys: Effects of microalloying and thermomechanical processing on microstructures and mechanical properties. *Mater. Design* **55**, 987–998 (2014).
- Kumpfert, J., Kim, Y. W. & Dimiduk, D. M. Effect of microstructure on fatigue and tensile properties of the gamma-TiAl alloy Ti-46.5Al-3.0Nb-2.1Cr-0.2W. *Mater. Sci. Eng. A* **192**, 465–473 (1995).
- Kamikawa, N., Huang, X., Tsuji, N. & Hansen, N. Strengthening mechanisms in nanostructured high-purity aluminium deformed to high strain and annealed. *Acta Mater.* **57**, 4198–4208 (2009).
- Zhang, Y., Zhou, Y. J., Lin, J. P., Chen, G. L. & Liaw, P. K. Solid-solution phase formation rules for multi-component alloys. *Adv. Eng. Mater.* **10**, 534–538 (2008).
- Guo, S., Hu, Q., Ng, C. & Liu, C. T. More than entropy in high-entropy alloys: Forming solid solutions or amorphous phase. *Intermetallics* **41**, 96–103 (2013).
- Guo, S., Ng, C. & Liu, C. T. Anomalous solidification microstructure in Co-free $\text{Al}_x\text{CrCuFeNi}_2$ high-entropy alloys. *J. Alloy. Compd.* **557**, 77–81 (2013).
- Zhang, F., Zhang, C., Chen, S. L., Zhu, J., Cao, W. S. & Kattner, U. R. An understanding of high entropy alloys from phase diagram calculations. *CALPHAD* **45**, 1–10 (2014).
- Zhang, C., Zhang, F., Chen, S. L. & Cao, W. S. Computational thermodynamics aided high-entropy alloy design. *JOM* **64**, 839–845 (2012).

Acknowledgments

This research was supported by the National Science Foundation of China (Nos. 51104029, U1332115 and 51134013), the Key grant Project of Chinese Ministry of Education (No.313011) and the Fundamental Research Funds for the Central Universities.

Author contributions

Y.L., S.G. and T.W. conceived the idea and designed the experiment. Y.D., L.J., H.K. and J.J. performed the experiments. B.W., Z.W., Z.C., H.R. and T.L. contributed to the results analysis and discussion. Y.L. and S.G. wrote the paper.

Additional information

Competing financial interests: The authors declare no competing financial interests.

How to cite this article: Lu, Y. *et al.* A Promising New Class of High-Temperature Alloys: Eutectic High-Entropy Alloys. *Sci. Rep.* **4**, 6200; DOI:10.1038/srep06200 (2014).



This work is licensed under a Creative Commons Attribution-NonCommercial-NoDerivs 4.0 International License. The images or other third party material in this article are included in the article's Creative Commons license, unless indicated otherwise in the credit line; if the material is not included under the Creative Commons license, users will need to obtain permission from the license holder in order to reproduce the material. To view a copy of this license, visit <http://creativecommons.org/licenses/by-nc-nd/4.0/>